Global atmospheric transport and source-receptor relationships for arsenic

Ka-Ming Wai[1], Shiliang Wu[1,2*], Xueling Li[2], Dan A. Jaffe[3], Kevin D. Perry[4]

[1]Dept. of Geological and Mining Engineering and Sciences, Michigan Technological University, Houghton, Michigan, USA

[2]Dept. of Civil and Environmental Engineering, Michigan Technological University, Houghton, Michigan, USA

[3]Physical Sciences Div., School of Science, Technology, Engineering and Mathematics, University of Washington Bothell, Bothell, Washington, USA

[4]Dept. of Atmospheric Sciences, University of Utah, Salt Lake City, Utah, USA

[*]e-mail: slwu@mtu.edu

Arsenic and many of its compounds are toxic pollutants in the global environment. They can be transported long distances in the atmosphere before depositing to the surface, but the global source-receptor relationships between various regions have not yet been assessed. We develop the first global model for atmospheric arsenic to better understand and quantify its inter-continental transport. Our model reproduces the observed arsenic concentrations in surface air over various sites around the world. The global arsenic emission inventory that we have developed shows a total arsenic emission of 30.7 Gg yr^{-1} of which more than 90% is derived from anthropogenic sources. The global average atmospheric lifetime of arsenic is calculated to be 4.5 days. Arsenic emissions from Asia and South America are found to be the dominant sources for atmospheric arsenic in the Northern and Southern Hemispheres, respectively. Asian emissions are found to contribute 39% and 38% of the total arsenic deposition over the Arctic and Northern America, respectively. Another 14% of the arsenic deposition to the Arctic region is attributed to European emissions. Our results indicate that the reduction of anthropogenic arsenic emissions in Asia and South America can significantly reduce arsenic pollution not only locally but also globally.

Arsenic is a ubiquitous metalloid in the global environment. Elemental arsenic and many of its compounds have high toxicity and have been listed by the International Agency for Research on Cancer (IARC) as Group 1 carcinogens[1]. They, even at relatively low exposure levels, can also cause many other adverse health effects related to the brain and nervous system, digestive system, and skin[2-6].

There have been increasing concerns about arsenic pollution in the environment. In 2012, Consumer Reports[7] conducted tests on more than 200 samples of rice products in the United States and found that many of them (including some organic products and infant rice cereals) contain arsenic at "worrisome levels". Since 2013, the European Union has set the standard for arsenic concentration in ambient air, which is 6 ng m^{-3} for annual mean concentrations.

There are large spatial variations for the atmospheric concentrations of arsenic, which can vary by several orders of magnitudes from less than 0.1 ng m^{-3} in remote sites to more than 10 ng m^{-3} in urban/industrial areas, presumably reflecting the impacts from anthropogenic activities. In the south polar atmosphere, the arsenic concentrations were reported to be less than 41 pg m^{-3} [8]. In China and Chile, the dominant arsenic source regions in the Northern and Southern Hemispheres, respectively, the arsenic concentrations were reported to reach 15 ng m^{-3} or higher[9,10]. The typical residence time of arsenic in the atmosphere is several days[11-13], making it capable of long-range transport. This implies that arsenic emissions from one region can significantly affect other regions downwind. However, the global source-receptor relationship between various regions has not been quantified so far.

There have been some studies on the regional atmospheric transport of arsenic. Pacyna et al.[14] and Akeredolu et al.[15] investigated the long-range transport of arsenic and other heavy metals from Europe to Norway and the Arctic region, respectively. Gidhagen et

al.[10] studied the regional effects from smelter emissions of arsenic in Chile. Based on the significant arsenic enrichment in snowpack samples from the Antarctic Plateau, Hong et al.[16] proposed that the emissions of trace elements (including arsenic) from nonferrous metal smelting and fossil fuel combustion processes in South America, especially in Chile, are the most likely sources.

There are both anthropogenic and natural sources for atmospheric arsenic. Metal (copper, zinc, and lead) smelting and coal combustion are the major anthropogenic arsenic sources[17-20], with copper smelting being the most important single source[13,18,19,20]. Additional minor anthropogenic sources include application of herbicide, wood preservation, and waste incineration[20]. Natural sources for arsenic in the atmosphere include volcanic emissions, wind erosion of soil, and biological activities, with volcanic emissions being the most important source[13,17, 21]. There are large uncertainties associated with the estimation of arsenic emissions to the atmosphere, but most studies have shown that for the present-day conditions, the global anthropogenic sources are much more dominant than natural sources[13,17,22,23].

In this study, we develop the first-ever global gridded emission inventory for arsenic (more details in the Methods section) and implement it in a global atmospheric chemical transport model (GEOS-Chem) to examine the global transport and source-receptor relationships for arsenic. The global arsenic emissions are calculated to be 30.7 Gg yr^{-1} with the breakdown for major source regions (15.8 and 4.4 Gg yr^{-1} in East Asia and South America, respectively) summarized in the Supplementary Information Table S1. Our

global total arsenic emission is comparable to previous studies by Walsh et al.[13] and Nriagu[21] who both estimated the global total arsenic emissions to be 31 Gg yr^{-1}. In contrast, Chilvers and Peterson[20] estimated a very large natural source for arsenic leading to a much higher global total arsenic emission of 73.5 Gg yr^{-1}. The model-simulated annual mean concentrations of atmospheric arsenic are compared with available measurement data in Fig. 1 and Table 1. We find very good agreement between model results and observations with a high correlation ($r^2 = 0.98$).

Figure 1 shows the annual average arsenic concentrations in ambient air driven by synoptic transport events. High arsenic concentrations (10 ng m^{-3} or higher) are found over large areas in eastern China and northern Chile (Fig. 1), which are at least one order of magnitude higher than those in the United States and Europe. Figure 1 also illustrates the outflow of arsenic plumes from Asia, which are transported over the North Pacific and North America following the Westerlies. Similarly the arsenic plumes from North America are transported across the North Atlantic towards Europe. In the Southern Hemisphere, the major arsenic source is Chile. The arsenic plumes at lower latitudes are transported towards the tropical Pacific following the trade winds, and those at higher latitudes are transported towards the Southern Atlantic following the Westerlies.

We further evaluate the model performance in simulating the daily time series of measured atmospheric arsenic concentrations at the Mt. Bachelor Observatory (MBO, 44.0° N, 121.7° W), located on the west coast of the United States (Fig. 2). This site has been used for over a decade to examine long-range transport of aerosol and gas phase

pollutants in baseline air arriving to North America[24,25]. The model reproduces the temporal variations in arsenic concentrations reasonably well ($r^2 = 0.35$).

In order to better examine the source-receptor relationships between various regions in terms of arsenic concentration and deposition, we carry out a suite of sensitivity simulations where anthropogenic arsenic emissions from a certain region are turned off in the model. For example, we shut off emissions from Asia in the sensitivity model run and then compare the calculated atmospheric arsenic deposition (D_{no_Asia}) with those from the base run (D_{base}) to derive the percentage contribution of Asian emissions to atmospheric arsenic in the receptor region: $Contribution_{Asia} = (D_{base} - D_{no\_Asia}) / D_{base} \times 100\%$. Figure 3 shows the contribution to total (wet + dry) deposition from each continental-scale source region. Similarly, the contributions to atmospheric arsenic concentration from the corresponding source regions are shown in the Supplementary Information Fig. S1.

Anthropogenic arsenic emissions from Asia are found to make the largest contributions to atmospheric arsenic deposition over the North Pacific Ocean and western North America (Fig. 3a). About 10-60% of atmospheric arsenic concentration and 30-70% of total arsenic deposition over the western part of North America are attributed to Asian emissions. Significant contributions to the Arctic region (up to 60% for atmospheric concentration and 70% for total arsenic deposition) are calculated for Asian emissions (Fig. 3a).

Figure 3b shows the contribution from European anthropogenic arsenic emissions. The European contributions mainly extend northward to the Arctic and eastward over part of Russia. The European emissions are also found to contribute to arsenic deposition over the Mediterranean Sea by up to 60%. Figure 3c shows the contribution from North American anthropogenic arsenic emissions. The eastward transport of the arsenic-laden plumes from North America leads to its large contribution to the arsenic deposition over the North Atlantic Ocean (up to 80% right off the eastern coast of the US).

The source-receptor relationships for atmospheric arsenic concentration and deposition between major regions in the Northern Hemisphere are summarized in Table 2. On average, about 39% of the total arsenic deposition over the Arctic region is attributed to Asian anthropogenic emissions, reflecting the strong arsenic emissions from Asia. The European anthropogenic emissions are calculated to contribute almost 14% of the total arsenic deposition to the Arctic. The North American contribution to arsenic in the Arctic (about 4%) is found to be much less than those from Asia or Europe, reflecting both the lower anthropogenic emission strengths and the lower latitudes of the sources. The Asian anthropogenic emissions are found to contribute to the total arsenic deposition in North America by 38%.

The contribution of anthropogenic arsenic emissions from South America is found to dominate over the Southern Hemisphere except for Southern Africa and Australia (Fig. 3d). Up to 90% of arsenic deposition over the Antarctic is attributed to emissions from South America, which confirms the hypothesis by Hong et al.[16].

The inter-continental transport of arsenic, especially the significant global impacts associated with arsenic emissions from certain source regions as shown by our results, highlights the benefits of international cooperation to reduce arsenic pollution around the world. These source-receptor relationships should be considered by researchers and policymakers in designing mitigation strategies for arsenic pollution.

Methods

Model Description. We developed a global arsenic model based on the GEOS-Chem chemical transport model (http://geos-chem.org) v9-01-01. The GEOS-Chem model has been applied to a wide range of research related to atmospheric trace gases, aerosols and mercury[S1-S3]. It is driven by assimilated meteorological fields from NASA GMAO. All references introduced in the Methods Section are detailed in the Supplementary Information.

Global Emissions Development. Available data on arsenic emissions for various regions around the world were compiled, processed and gridded to 4^{o} latitude by 5^{o} longitude for the model with a base year of 2005 (unless otherwise specified). For Chile, the major arsenic source region in the Southern Hemisphere, we followed Gidhagen et al.[10]. The Australian emissions were based on Australia's National Pollutant Inventory (NPI) (http://www.npi.gov.au/resource/arsenic-and-compounds-0). Arsenic emissions in the United States followed the U.S. EPA NATA (National-Scale Air Toxics Assessment) inventory for 1999 (http://www.epa.gov/ttn/atw/nata1999/index.html). The Canadian

emissions were based on Environment Canada's National Pollutant Release Inventory (NPRI) (http://www.ec.gc.ca/inrp-npri). The European emissions of arsenic followed the ESPREME inventory (http://espreme.ier.uni-stuttgart.de).

There is no national emission inventory for arsenic emissions from metal smelting available for China, so we developed a new inventory for China in this study. It was derived using the production data of non-ferrous metals from the *Yearbook of Nonferrous Metals Industry of China 2005*[S4] and the corresponding arsenic emission factors from Chilvers and Peterson[20]. Arsenic emissions from coal-fired power plants in China followed Tian et al.[S5]. Initial model evaluation with our a priori arsenic emission inventory developed for China showed a systematic low bias for model-simulated arsenic concentrations over China. A likely reason for this low bias is that the arsenic emission factors[20] from metal smelting used in this study might be too low for China. So we scaled up the arsenic emissions due to metal smelting in China by a factor of 1.5 and then found very good agreement between model results and observational data (Fig. 1).

Anthropogenic arsenic emissions from other countries around the world were estimated by taking advantage of the available SO_2 emission inventories from the Emissions Database for Global Atmospheric Research (EDGAR; http://edgar.jrc.ec.europa.eu). We followed EDGAR version 3[S6] for SO_2 emissions in 2005 and applied a median value of 5.63×10^{-4} g As/g S for As/S emission ratios[S7,S8] to derive the arsenic emissions from other countries not previously mentioned.

196 We also estimated arsenic emissions from volcanic activities based on the As/S
197 correlations. We followed the global volcanic SO_2 emission inventory from Andres and
198 Kasgnoc[S9] and the volcanic arsenic emissions were calculated using the ratio of 1.59 x
199 10^{-4} g As/g S, which is the median value of As/S flux ratios found for volcanic emissions
200 around the world[S10-S13].
201
202 Because the absolute majority of atmospheric arsenic sorbs onto aerosols[18], we treated
203 the deposition processes of arsenic similarly as $PM_{2.5}$ aerosols. The wet deposition of
204 arsenic followed the scheme used by Liu et al.[S14], which considers the scavenging from
205 convective updrafts, rainout from convective anvils and rainout and washout from large-
206 scale precipitation. The dry deposition followed a resistance-in-series scheme[S15], with the
207 surface resistances following the work of Zhang et al.[S16]. The global total wet and dry
208 deposition of arsenic was calculated to be 25.4 Gg yr^{-1} and 5.3 Gg yr^{-1}, respectively.
209
210 The global total atmospheric burden of arsenic is calculated to be 377 Mg leading to a
211 global average atmospheric lifetime for arsenic of 4.5 days. The calculated atmospheric
212 arsenic lifetimes against deposition range from 4.1 to 5.4 days for different regions
213 around the world (Table S1), which are within the range (2.5 – 9 days) reported in the
214 literature[11-13].
215
216 For model evaluation, we focused on atmospheric arsenic measurement data from
217 nonurban sites given the coarse spatial resolution (4^o latitude x 5^o longitude) of the global
218 model. We collected available measurement data from various regions around the world

219 in the literature and compiled them in Table 1. Except for the time series data from the
220 Mt. Bachelor Observatory, data for sites in the United States and Europe were from the
221 Interagency Monitoring of Protected Visual Environments (IMPROVE) and the European
222 Monitoring and Evaluation Programme (EMEP) network, respectively. Data from the
223 MBO were obtained using a rotating drum impactor with 3-hour time resolution and with
224 synchrotron X-ray fluorescence analysis[25].
225
226
227

Acknowledgement

The authors thank the EMEP data providers for making the arsenic data available. This publication was made possible by a U.S. EPA grant (grant 83518901). Its contents are solely the responsibility of the grantee and do not necessarily represent the official views of the U.S. EPA. Further, the U.S. EPA does not endorse the purchase of any commercial products or services mentioned in the publication. S.W. acknowledges support from the NSF (grant 1313755). The Mt. Bachelor Observatory is supported by the NSF (grant 1447832).

Author contributions

K.M.W. and S.W. designed the entire study and wrote the manuscript. K.M.W. developed the arsenic model based on the standard GEOS-Chem model and did all model experiments and analysis of outputs. X.L. assisted the project with literature review and database preparation at the early stage of the project. D.A.J. and K.D.P. provided data of atmospheric arsenic measurements from Mt. Bachelor Observatory, USA.

Competing financial interests

The authors declare no competing financial interests.

References

1. IARC (International Agency for Research on Cancer). IARC Monographs on the evaluation of carcinogenic risks to humans (2013) (Available at: http://monographs.iarc.fr/ENG/Classification).
2. Navas-Acien, A., Silbergeld, E. K., Pastor-Barriuso, R. & Guallar, E. Arsenic exposure and prevalence of type 2 diabetes in US adults. *JAMA* **300**, 814–822 (2008).
3. Ettinger, A. S., *et al.* Maternal arsenic exposure and impaired glucose tolerance during pregnancy. *Environ. Health. Perspect.* **117**, 1059–1064 (2009).
4. European Food Safety Authority. EFSA J. EFSA Panel on Contaminants in the Food Chain (CONTAM); scientific opinion on arsenic in food (2009) (Available at: http://www.efsa.europa.eu/en/scdocs/scdoc/1351.htm).
5. Sohel, N., *et al.* Arsenic in drinking water and adult mortality: a population-based cohort study in rural Bangladesh. *Epidemiology* **20**, 824–830 (2009).
6. Leonardi, G., *et al.* Arsenic and basal cell carcinoma in areas of Hungary, Romania, and Slovakia: a case–control study. *Environ. Health Perspect.* **120**, 721–726 (2012).
7. Consumer Reports. Arsenic in your food (2012) (Available at: http://www.consumerreports.org/cro/magazine/2012/11/arsenic-in-your-food/index.htm).
8. Maenhaut, W., Zoller, W. H., Duce, R. A. & Hoffman, G. L. Concentration and size distribution of particulate trace elements in the south polar atmosphere. *J. Geophys. Res.* **84**, 2421–2431 (1979).
9. Li, C. *et al.* Concentrations and origins of atmospheric lead and other trace species at a rural site in northern China. *J. Geophys. Res.***115**, D00K23 (2010).
10. Gidhagen, L., Kahelin, H., Schmidt-Thomé, P. & Johansson, C. Anthropogenic and natural levels of arsenic in PM_{10} in Central and Northern Chile. *Atmos. Environ.* **36**, 3803–3817 (2002).
11. Pacyna, J. M. In *Lead, Mercury, Cadmium and Arsenic in the Environment SCOPE 31 Ch. 7*

(eds. Hutchinson, T. C. & Meema, K. M.) (John Wiley & Sons, Chichester, 1987).

12. DET - Department of the Environment, Transport and the Regions, Scottish Executive, The National Assembly for Wales. A review of arsenic in ambient air in the UK (2000) (Available at http://uk-air.defra.gov.uk/reports/empire/arsenic00/arsenic_97v.pdf).
13. Walsh, P. R., Duce, R. A. & Fasching, J. L. Considerations of the enrichment, sources, and flux of arsenic in the troposphere. *J. Geophys. Res.* **84**, 1719–1726 (1979).
14. Pacyna, J. M., Bartonova, A., Cornille, P. & Maenhaut, W. Modelling of long-range transport of trace elements. A case study. *Atmos. Environ.* **23**, 107–114 (1989).
15. Akeredolu, F. A. *et al.* The flux of anthropogenic trace metals into the arctic from the mid-latitudes in 1979/80. *Atmos. Environ.* **28**, 1557–1572 (1994).
16. Hong, S. *et al.* Evidence of Global-Scale As, Mo, Sb, and Tl Atmospheric Pollution in the Antarctic Snow. *Environ. Sci. Tech.* **46**, 11550–11557 (2012).
17. WHO (World Health Organization). *Air Quality Guidelines Second Edition* (WHO Regional Office for Europe, Copenhagen, Denmark, 2000).
18. Deschamps, E. & Matschullat, J. In *Arsenic : natural and anthropogenic* (eds. Deschamps, E. & Matschullat, J.) (CRC Press, Boca Raton, Florida, USA, 2011).
19. Brimblecombe, P. Atmospheric arsenic. *Nature* **280**, 104–105 (1979).
20. Chilvers, D. C. & Peterson, P. J. In *Lead, Mercury, Cadmium and Arsenic in the Environment SCOPE 31 Ch. 17* (eds. Hutchinson, T. C. & Meema, K. M.) (John Wiley & Sons, Chichester, 1987).
21. Nriagu, J. O. A global assessment of natural sources of atmospheric trace metals. *Nature* **338**, 47–49 (1989).
22. Galloway, J. N., Thornton, J. D., Norton, S. A., Volchok, H. L. & McLean, R. A. N. Trace metals in atmospheric deposition: A review and assessment. *Atmos. Environ.* **16**, 1677–1700 (1982).
23. Shotyk, W., Cheburkin, A. K., Appleby, P. G., Fankhauser, A. & Kramers, J. D. Two thousand

years of atmospheric arsenic, antimony, and lead deposition recorded in an ombrotrophic peat bog profile, Jura Mountains, Switzerland. *Earth Planet. Sci. Lett.* **145**, E1–E7 (1996).

24. Jaffe, D. A. *et al.* Export of Atmospheric Mercury from Asia. *Atmos. Environ.* **39**, 3029-3038 (2005).
25. Fischer, E.V., Perry, K. D. & Jaffe, D. A. Optical and chemical properties of aerosols transported to Mount Bachelor during spring 2010. *J. Geophys. Res.* **116**, D18202 (2011).
26. Chen, J. *et al*. Characteristics of trace elements and lead isotope ratios in $PM_{2.5}$ from four sites in Shanghai. *J. Hazard. Mat.* **156**, 36–43 (2008).
27. Yang, Y. *et al.* Elemental composition of $PM_{2.5}$ and PM_{10} at Mount Gongga in China during 2006. *Atmos. Res.* **93**, 801–810 (2009).
28. Kang, J. *et al*. A five-year observation of atmospheric metals on Ulleung Island in the East/Japan Sea: Temporal variability and source identification. *Atmos. Environ.* **45**, 4252–4262 (2011).

Figure Legends

Figure 1 | Arsenic concentrations in surface air. Model-simulated annual mean arsenic concentrations (background) in ambient air compared with measurement data at various stations (circles) around the world.

Figure 2 | Daily arsenic concentrations in spring 2011. Measured daily average arsenic concentrations at the Mt. Bachelor Observatory (located on the west coast of the United States) compared with model results.

Figure 3 | Source attribution for arsenic deposition. Percent contributions to total arsenic deposition from: (a) Asia; (b) Europe; (c) North America; and (d) South America.

330

Table 1| Model-simulated annual average surface atmospheric arsenic concentrations compared with observations.

Site	Model result (ng m^{-3})	Observations (ng m^{-3})	Year of observations	Source for observational data
Storhofdi, Iceland (63.4° N, 20.3° W)	0.07	0.18	2005	EMEP
Peyrusse Vieille, France (43.6° N, 0.2° E)	0.14	0.20	2005	EMEP
Neuglobsow, Germany (53.1° N, 13.0° E)	0.47	0.86	2005	EMEP
Topoliniky, Slovakia (48.0° N, 17.8° E)	0.84	0.44	2005	EMEP
Montseny, Spain (41.8° N, 2.4° E)	0.20	0.29	2005	EMEP
Bredkalen, Sweden (63.8° N, 15.3° E)	0.09	0.10	2002	EMEP
Pallas, Finland (61.0° N, 24.2° E)	0.27	0.15	2005	EMEP
Rucava, Latvia (56.2° N, 21.1° E)	0.27	0.38	2005	EMEP
Florida, US (30.1° N, 84.2	0.48	0.46	2005	IMPROVE

° W)				
Virginia, US (37.6° N, 79.5° W)	0.63	0.44	2005	IMPROVE
Maine, US (46.7° N, 68.0 ° W)	0.25	0.16	2005	IMPROVE
Michigan, US (47.5° N, 88.1° W)	0.19	0.15	2004	IMPROVE
South Dakota, US (43.7° N, 101.9° W)	0.14	0.05	2005	IMPROVE
Texas, US (31.8° N, 104.8 ° W)	0.23	0.23	2005	IMPROVE
Washington, US (46.6° N, 121.4° W)	0.18	0.12	2005	IMPROVE
California, US (34.2° N, 116.9° W)	0.18	0.07	2005	IMPROVE
Idaho, US (44.2° N, 114.9 ° W)	0.19	0.03	2005	IMPROVE
Hawaii, US (19.4° N, 155.3° W)	0.10	0.01	2005	IMPROVE
Alaska1, US (56.5° N, 132.8° W)	0.07	0.02	2005	IMPROVE
Alaska2, US (55.3° N,	0.08	0.04	2005	IMPROVE

160.5° W)				
Beijing, China (39.8° N, 117.0° E)	22	18	2005	[9]
Shanghai, China (31.4° N, 121.3° E)	26	27	2004-2005	[26]
Sichuan, China (29.6° N, 102.0° E)	4.2	6.1	2006	[27]
Ulleung Island, S. Korea (37.5° N, 130.9° E)	3.6	3.0	2003-2008	[28]
Quillota, Chile (32.9° S, 71.2° W)	30	31	1999-2000	[10]
Quillagua, Chile (21.6° S, 69.5° W)	4.4	6.5	1999-2000	[10]

335

Table 2| Source-receptor relationships for atmospheric arsenic concentration (deposition) between various regions*.

		Source regions		
		Asia	Europe	North America
Receptor regions	Arctic (66 – 90°N, 179°W – 179°E)	24.9 (39.2)	14.2 (13.8)	3.9 (4.3)
	Asia (10 – 70°N, 60 – 145°E)	56.3 (58.0)	4.3 (4.9)	0.1 (0.2)
	Europe (35 – 70°N, 5°W – 60°E)	6.4 (10.0)	68.6 (60.1)	1.3 (2.0)
	North America (30 – 70°N, 125 – 65°W)	25.7 (38.2)	2.0 (1.1)	55.1 (41.4)
	Western US (30 – 48°N, 125 – 100°W)	36.0 (48.3)	0.4 (0.4)	45.9 (30.0)
	Eastern US (30 – 48°N, 100 – 70°W)	8.9 (16.3)	0.2 (0.2)	85.0 (67.7)

*Shown as the percentage contribution to total atmospheric arsenic concentration (deposition) in the receptor region from the source region.

336

337

338

339

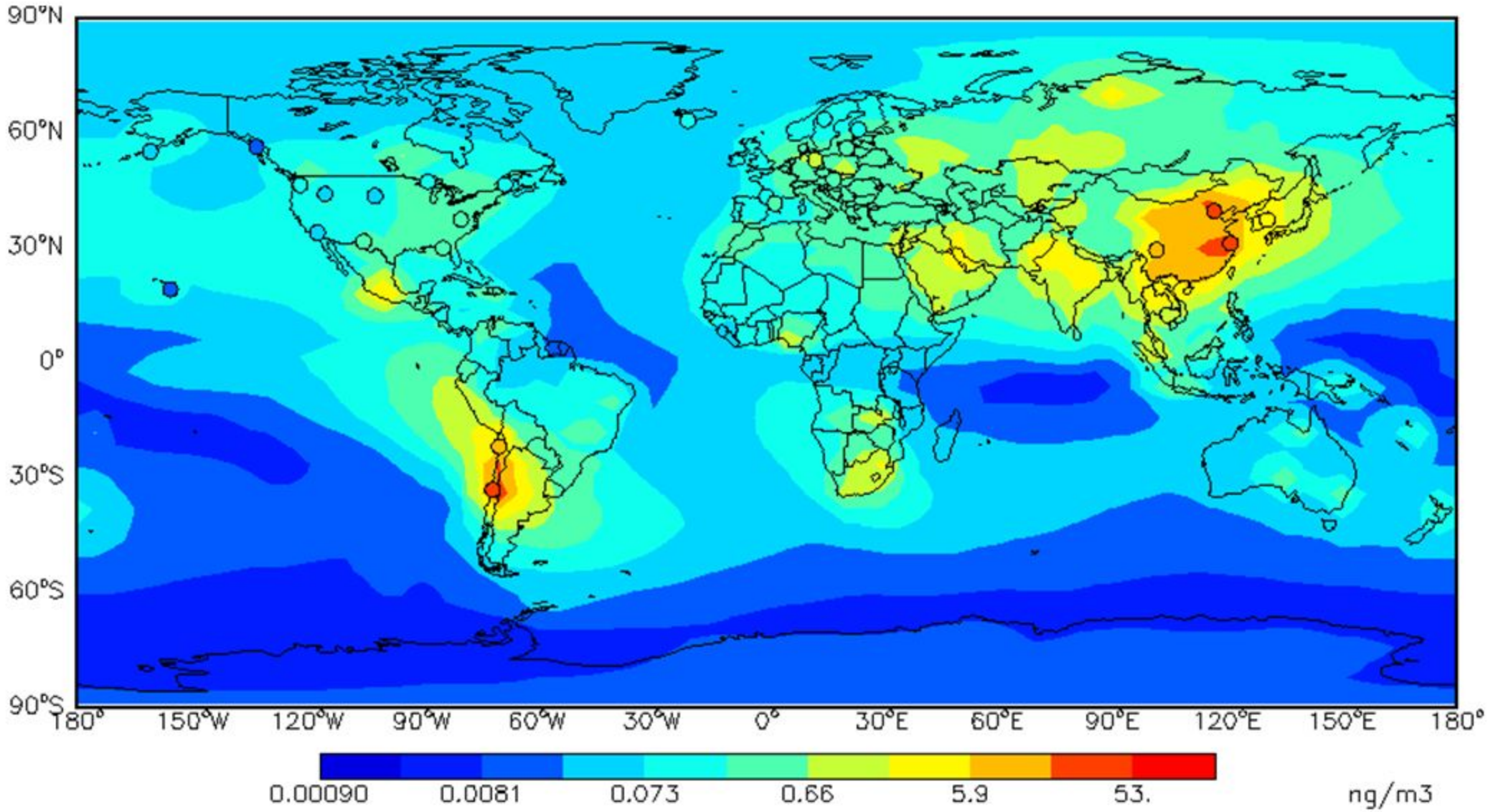
90°N
60°N
30°N
0°
30°S
60°S
90°S
180°
150°W
120°W
90°W
60°W
30°W
0°
30°E
60°E
90°E
120°E
150°E
180°
0.00090
0.0081
0.073
0.66
5.9
53.
ng/m3

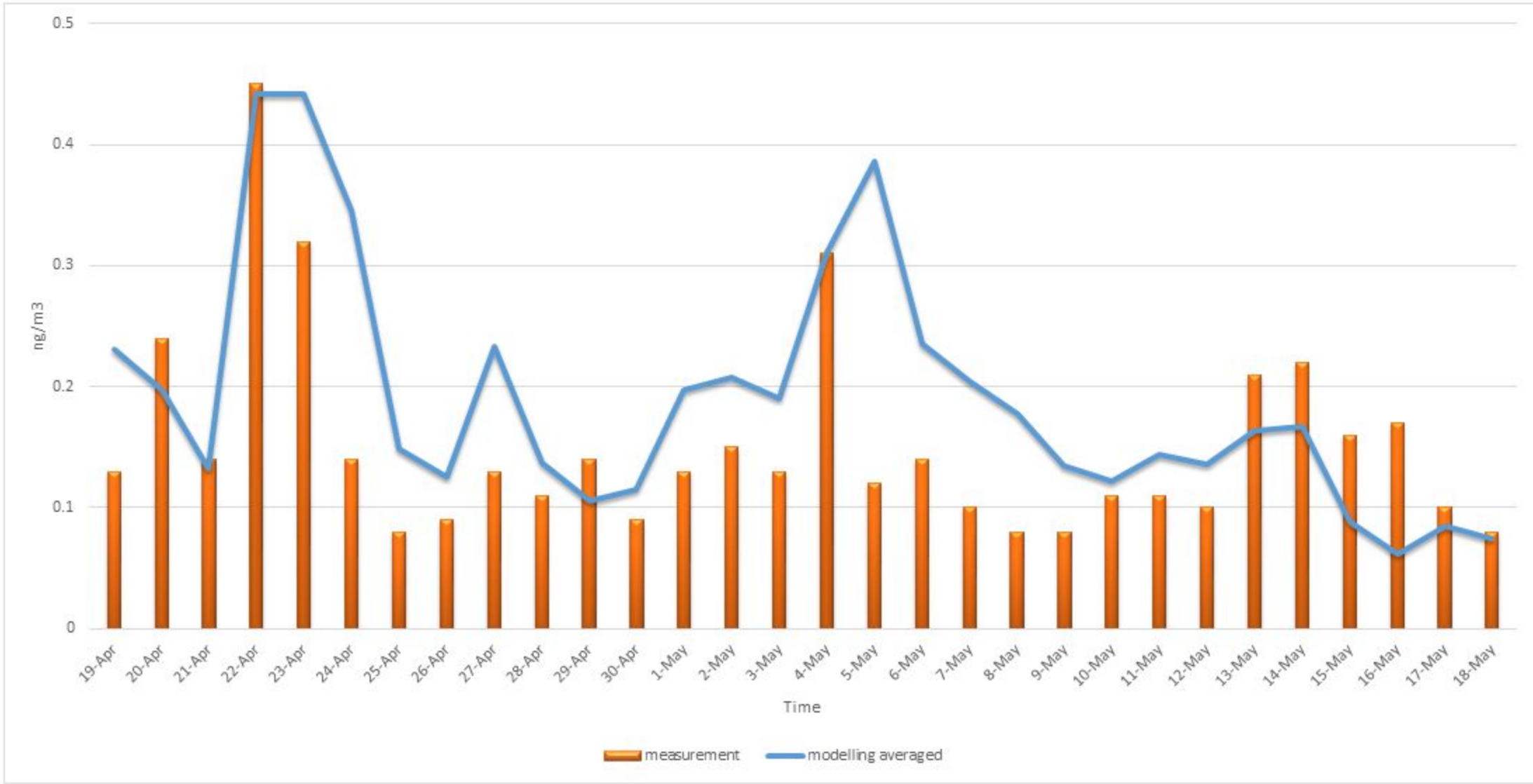
0.5
0.4
0.3
0.2
0.1
0
ng/m3
19-Apr
20-Apr
21-Apr
22-Apr
23-Apr
24-Apr
25-Apr
26-Apr
27-Apr
28-Apr
29-Apr
30-Apr
1-May
2-May
3-May
4-May
5-May
6-May
7-May
8-May
9-May
10-May
11-May
12-May
13-May
14-May
15-May
16-May
17-May
18-May
Time
measurement
modelling averaged

a)

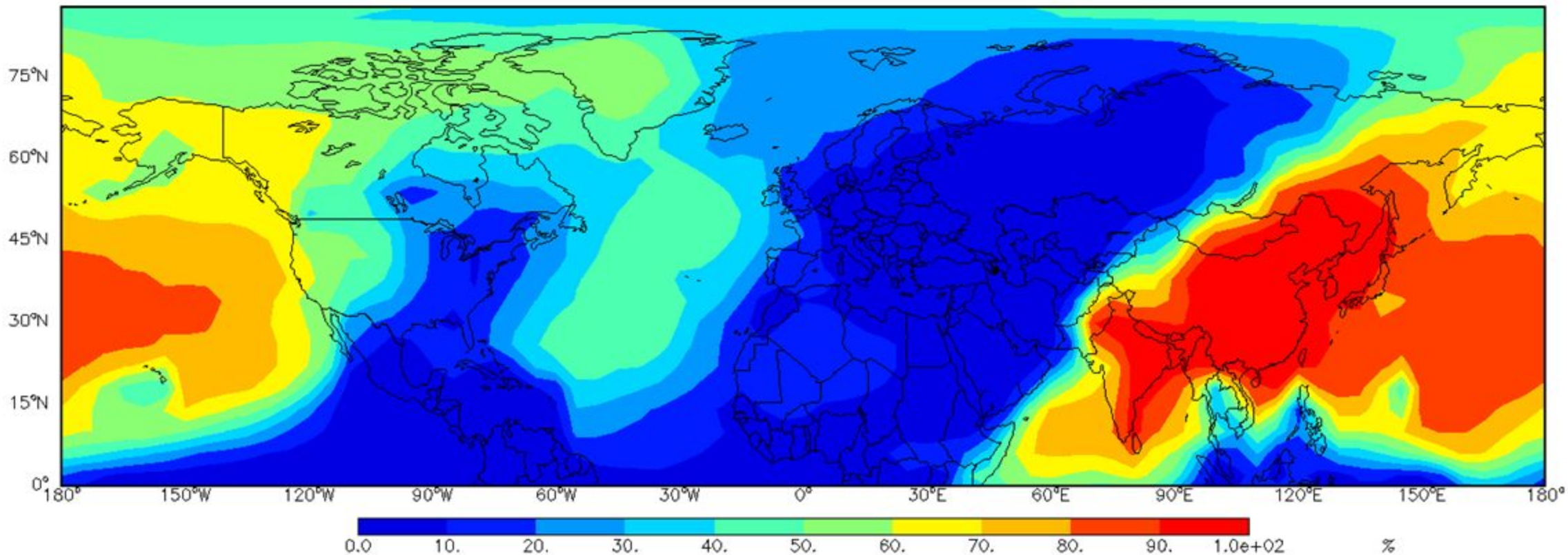
75°N
60°N
45°N
30°N
15°N
0°
180°
150°W
120°W
90°W
60°W
30°W
0°
30°E
60°E
90°E
120°E
150°E
180°
0.0
10.
20.
30.
40.
50.
60.
70.
80.
90.
1.0e+02
%

b)

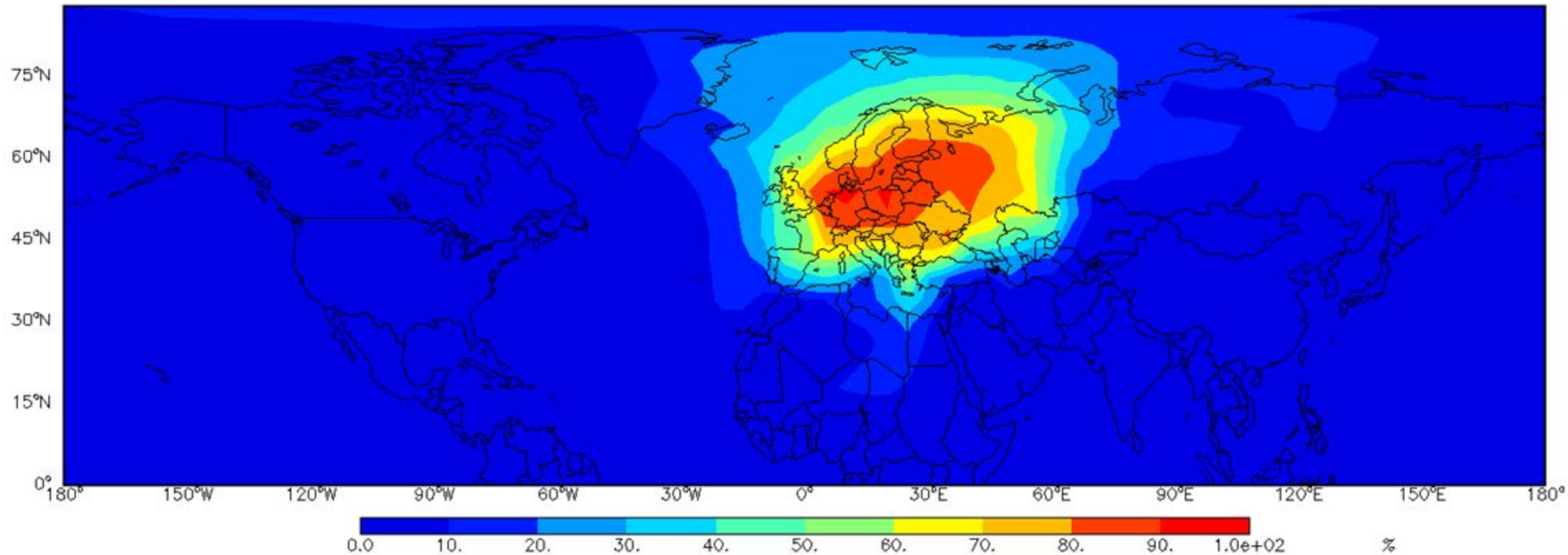
75°N
60°N
45°N
30°N
15°N
0°
180°
150°W
120°W
90°W
60°W
30°W
0°
30°E
60°E
90°E
120°E
150°E
180°
0.0
10.
20.
30.
40.
50.
60.
70.
80.
90.
1.0e+02
%

c)

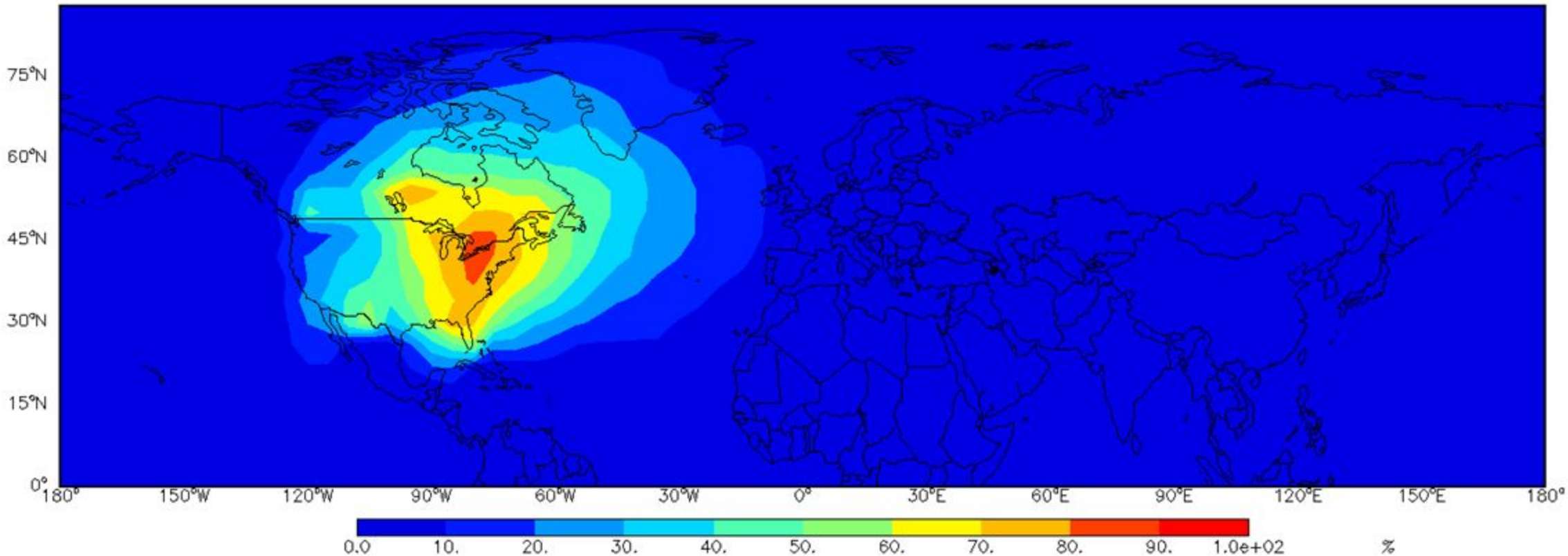
75°N
60°N
45°N
30°N
15°N
0°
180°
150°W
120°W
90°W
60°W
30°W
0°
30°E
60°E
90°E
120°E
150°E
180°
0.0
10.
20.
30.
40.
50.
60.
70.
80.
90.
1.0e+02
%

d)

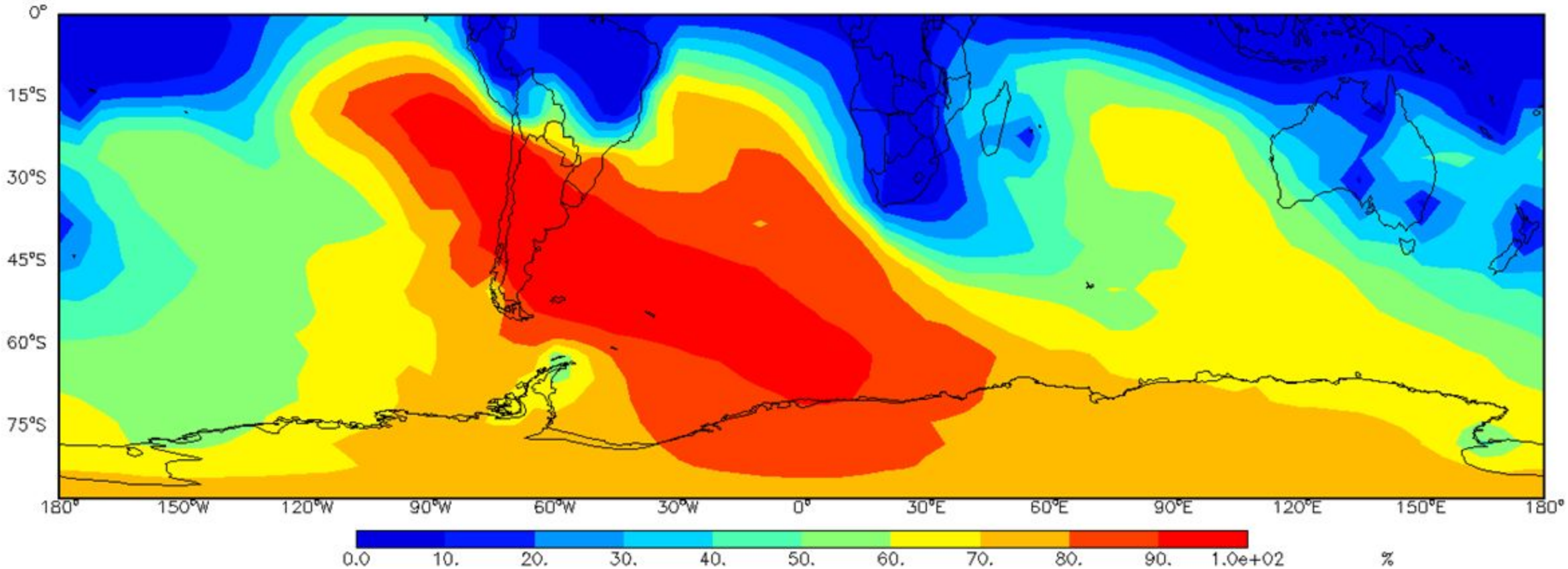
0°
15°S
30°S
45°S
60°S
75°S
180°
150°W
120°W
90°W
60°W
30°W
0°
30°E
60°E
90°E
120°E
150°E
180°
0.0
10.
20.
30.
40.
50.
60.
70.
80.
90.
1.0e+02
%